Decomposition of M-ary CPM Signals into PAM Waveforms

Umberto Mengali, *Fellow, IEEE*, and Michele Morelli

***Abstract*—It is widely known that minimum shift keying (MSK) may be seen as a PAM signaling scheme and that the same is true, albeit approximately, with MSK-like modulations. It is also known (perhaps not so widely) that any *binary* continuous phase-modulated (CPM) signal may be exactly decomposed into the sum of a few PAM waveforms. In this paper we show that this property extends to *multilevel* CPM signaling. Features of a PAM decomposition are discussed as a function of the alphabet size, the modulation index, and the frequency response of the system. It is found that, especially with signaling schemes with a long memory, the decomposition has so many terms that it becomes unmanageable. For these cases an approximation is proposed with a limited number of terms.**

***Index Terms*—Continuous phase modulation (CPM), MSK-like modulations.**

I. Introduction

CONTINUOUS phase modulation (CPM) forms a class of signaling formats that are efficient in power and bandwidth [1]. Furthermore, it generates constant envelope waveforms and therefore is very useful in radio channels employing nonlinear amplifiers. Notwithstanding these favorable features, however, current CPM applications are still limited to few simple cases (basically, MSK and its generalizations) because of implementation complexity and synchronization problems.

Implementation complexity has two separate aspects. One arises from the large number of states that are required to describe a CPM signal. As a consequence, a maximum-likelihood (ML) detector consists of a Viterbi algorithm operating on a possibly large trellis [2, ch. 8]. Methods to reduce the trellis size are discussed in [3]–[5]. The other aspect originates from the filter bank needed to calculate the optimum metrics for the ML detector (either coherent or noncoherent). Here, the number of filters equals the dimensionality of the signal space, which may be quite large for many efficient CPM formats. Methods to cut down this number without sacrificing error performance are discussed in [6]–[8]. Finally, synchronization is a much more difficult task than in linear modulations. Various strategies have been proposed to recover carrier phase and symbol timing from CPM signals. For example, in [2, ch. 9], [9], [10], a nonlinear circuit is used to extract tones at carrier and clock frequencies from the received waveform. With smoothed phase pulses and multilevel signaling, however, this method fails because the amplitude of the tones is too small compared to the noise level.

While most of the above problems seem deeply rooted into the very features of CPM schemes (continuous phase variation, constant envelope, etc.), their solution is hindered by the nonlinear nature of these modulations. Perhaps it is not coincidental that the so-called MSK-type signals, which may be viewed as (approximate) linear modulations [11], [12], are much easier to deal with in terms of receiver complexity and synchronization functions.

In a paper published in 1986, Laurent [13] has opened the way to a "linear" representation of CPM modulations. Actually he has shown that a *binary* CPM signal can be decomposed into the sum of a few pulse amplitude-modulated (PAM) waveforms. Laurent's decomposition (LD) has been used to reduce the size of the filter bank in coherent CPM detectors [7] and to find new phase recovery methods [14] for coherent detection. More recently, it has been exploited for carrier frequency recovery [15]. Unfortunately, LD is only valid for binary signaling and, as such, is restricted to a subset of CPM formats. The purpose of the present paper is to extend the LD to multilevel signaling.

The paper is organized in the following way. In the next section we overview LD for a binary alphabet. The results are exploited in Section III as a building block for extending LD to multilevel schemes. The key idea is that an M-ary signal may be viewed as the product of P binary waveforms (P on the order of $\log_2 M$). Performing the product of such waveforms leads to a sum of PAM components. Examples are provided in Section IV to illustrate the method. Since the number of PAM components may be large, especially with partial response schemes, the problem of discarding the less significant ones arises. This issue is addressed in Section V where mean-squared approximation methods are adopted. A few examples are discussed in Section VI. Finally, in Section VII, we draw the conclusions.

II. Laurent Decomposition for Binary Signals

A. CPM Signal Model

The complex envelope of a CPM signal has the form

$$s(t, \boldsymbol{\alpha}) = e^{j\psi(t, \boldsymbol{\alpha})} \tag{1}$$

with

$$\psi(t, \boldsymbol{\alpha}) = 2h\pi \sum_i \alpha_i q(t - iT). \tag{2}$$

Manuscript received July 14, 1994; revised Feb. 24, 1995.

The authors are with Dipartimento di Ingegneria della Informazione, Università di Pisa, 56100 Pisa, Italy.

IEEE Log Number 9413433.

Here h is the *modulation index*, T is the signaling interval, $\boldsymbol{\alpha} = \{\alpha_i\}$ are information data belonging to the M-ary alphabet $\{\pm 1, \pm 3, \cdots, \pm(M-1)\}$, and $q(t)$ is the so-called *phase response* of the system, which is related to the *frequency response* $f(t)$ by the relationship

$$q(t) = \int_{-\infty}^{t} f(\tau)\, d\tau. \tag{3}$$

The pulse $f(t)$ in (3) is time-limited to the interval $(0, LT)$ and satisfies the conditions

$$f(t) = f(LT - t) \tag{4}$$

$$\int_0^{LT} f(\tau)\, d\tau = q(LT) = \frac{1}{2}. \tag{5}$$

In numerical examples to be discussed later we consider frequency responses of rectangular shape. They are customarily indicated with the acronym $LREC$.

B. Laurent Decomposition

In [13] it has been shown that, with a binary alphabet ($\alpha_i = \pm 1$), the right-hand side of (1) may be expressed as a superposition of PAM waveforms

$$s(t, \boldsymbol{\alpha}) = \sum_{k=0}^{Q-1} \sum_{n} b_{k,n} c_k(t - nT) \tag{6}$$

where $Q = 2^{L-1}$ and $c_k(t)$ is given by

$$c_k(t) = \prod_{i=0}^{L-1} u(t + iT + \beta_{k,i} LT), \qquad 0 \le k \le Q-1. \tag{7}$$

Here the function $u(t)$ is defined as

$$u(t) = \begin{cases} \sin[2h\pi q(t)]/\sin(h\pi), & 0 \le t \le LT \\ u(2LT - t), & LT < t \le 2LT \\ 0, & \text{elsewhere} \end{cases} \tag{8}$$

and the parameters $\beta_{k,i}$ take on values 0 or 1. In particular $\beta_{k,0}$ is always zero while, for any integer i in the interval $1 \le i \le L-1$, $\beta_{k,i}$ is the ith bit in the radix-2 representation of k, i.e.

$$k = \sum_{i=1}^{L-1} 2^{i-1} \beta_{k,i}, \qquad 0 \le k \le Q-1. \tag{9}$$

Finally, the coefficients $b_{k,n}$ in (6) (henceforth referred to as *pseudo-symbols*) are related to the information data α_i by the relationship

$$b_{k,n} = \exp\left\{ jh\pi \left[\sum_{m=-\infty}^{n} \alpha_m - \sum_{i=0}^{L-1} \alpha_{n-i} \beta_{k,i} \right] \right\}. \tag{10}$$

The following remarks are of interest:

1) The nonlinear relationship (10) between pseudo-symbols and information data reflects the nonlinear nature of CPM modulations. Indeed, $s(t, \boldsymbol{\alpha})$ is a nonlinear function of the information data even if it depends linearly on the pseudo-symbols.

2) With *full response* systems ($L = 1$) Q is unity and there is only one PAM component in (6). With *partial response* systems ($L > 1$), instead, Q may be large. In many cases, however, the signal power is concentrated in the first PAM component, i.e., the one associated with the zero-order pulse

$$c_0(t) = \prod_{i=0}^{L-1} u(t + iT). \tag{11}$$

3) The generic pulse $c_k(t)$ is time limited to the interval $0 \le t \le D_k T$, where D_k is given by [13]

$$D_k = \min_i \{L(2 - \beta_{k,i}) - i\}, \qquad 0 \le i \le L-1. \tag{12}$$

In particular, it can be shown that

$$\begin{aligned} D_0 &= L + 1 \\ D_1 &= L - 1 \\ D_2 &= D_3 = L - 2 \\ D_4 &= D_5 = D_6 = D_7 = L - 3 \\ &\cdots \\ D_{Q/2} &= \cdots = D_{Q-1} = 1. \end{aligned} \tag{13}$$

4) In general, the pseudo-symbols $b_{k,n}$ are correlated, even if the information data are not. Assuming uncorrelated data, the pseudo-symbol correlations

$$B_{i,j}(q) = E\{b_{i,k} b^*_{j,k+q}\}$$

are given by

$$B_{i,j}(q) = B_{j,i}(-q) = [\cos(h\pi)]^{\Delta(i,j,q)} \tag{14}$$

with

$$\Delta(i, j, q) = |q| + \sum_{k=0}^{L-1} (\beta_{i,k} + \beta_{j,k}) - 2\left[\sum_{\substack{k \le -q-1 \\ k \le L-1 \\ k \ge 0}} \beta_{i,k} + \sum_{\substack{k \le q-1 \\ k \le L-1 \\ k \ge 0}} \beta_{j,k} + \sum_{\substack{k \le L-q-1 \\ k \le L-1 \\ k \ge 0 \\ k \ge 1-q}} \beta_{i,k} \cdot \beta_{j,k+q} \right]. \tag{15}$$

Here, the notation ($k \le a,\ k \le b$) means $k \le \min(a, b)$ and, likewise, ($k \ge a,\ k \ge b$) means $k \ge \max(a, b)$.

5) If h is an integer, the denominator of $u(t)$ in (8) vanishes and the Laurent decomposition seems to fail. We shall see later how to deal with these pathological cases.

III. LD Extension to Multilevel Signaling

A. Decomposition of an M-ary Sequence into Binary Subsequences

The key idea to extend the LD to multilevel modulations is to express the M-ary data sequence $\{\alpha_i\}$ in terms of binary subsequences. As we shall see, this allows us to write the multilevel signal as a product of binary CPM waveforms. Applying LD to each waveform leads to the desired result.

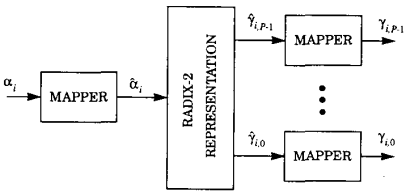

Fig. 1. Decomposition of an M-ary data sequence into binary subsequences.

To proceed, we call P that integer satisfying the conditions

$$2^{P-1} < M \leq 2^P \tag{16}$$

and we consider the mapping $\alpha \rightarrow \hat{\alpha}$ defined by

$$\hat{\alpha}_i = \frac{\alpha_i + 2^P - 1}{2}. \tag{17}$$

Clearly, as α_i varies in the set $\{\pm 1, \pm 3, \cdots, \pm(M-1)\}$, $\hat{\alpha}_i$ takes on values in the range

$$\frac{2^P - M}{2} \leq \hat{\alpha}_i \leq \frac{2^P + M}{2} - 1 \tag{18}$$

which, because of (16), may also be written as

$$0 \leq \hat{\alpha}_i \leq 2^P - 1. \tag{19}$$

It follows that $\hat{\alpha}_i$ may be represented in radix-2 form as

$$\hat{\alpha}_i = \sum_{l=0}^{P-1} \hat{\gamma}_{i,l} 2^l, \qquad \hat{\gamma}_{i,l} \in \{0, 1\}. \tag{20}$$

Next, elimination of $\hat{\alpha}_i$ from (17) and (20) yields

$$\alpha_i = 2 \sum_{l=0}^{P-1} \hat{\gamma}_{i,l} 2^l - (2^P - 1). \tag{21}$$

On the other hand, it may be checked that

$$2^P - 1 = \sum_{l=0}^{P-1} 2^l. \tag{22}$$

Thus (21) becomes

$$\alpha_i = \sum_{l=0}^{P-1} \gamma_{i,l} 2^l \tag{23}$$

where the coefficients $\gamma_{i,l}$ are related to $\hat{\gamma}_{i,l}$ by the mapping $\hat{\gamma} \rightarrow \gamma$

$$\gamma_{i,l} = 2\hat{\gamma}_{i,l} - 1 \qquad \gamma_{i,l} \in \{\pm 1\}. \tag{24}$$

As illustrated in Fig. 1, (17), (20), and (24) describe a method to transform an M-ary sequence $\{\alpha_i\}$ into P binary subsequences $\{\gamma_{i,l}\}$ $(0 \leq l \leq P-1)$. It is easily seen that the subsequences are independent if $\{\alpha_i\}$ is so and M equals 2^P. Table I provides an example of the above transformation for $M = 4$.

Inserting (23) into (1) and (2) yields

$$s(t, \boldsymbol{\alpha}) = \prod_{l=0}^{P-1} \exp\left\{ j 2h^{(l)} \pi \sum_i \gamma_{i,l} q(t - iT) \right\} \tag{25}$$

TABLE I
DECOMPOSITION FOR $M = 4$

α_i	$\hat{\alpha}_i$	$\hat{\gamma}_{i,1}$	$\hat{\gamma}_{i,0}$	$\gamma_{i,1}$	$\gamma_{i,0}$
-3	0	0	0	-1	-1
-1	1	0	1	-1	1
1	2	1	0	1	-1
3	3	1	1	1	1

with $h^{(l)} = 2^l h$. As anticipated, this equation indicates that an M-level CPM signal may be written as the product of P binary CPM waveforms.

B. Extension of Laurent Decomposition

Application of LD to each binary waveform in (25) yields

$$s(t, \boldsymbol{\alpha}) = \prod_{l=0}^{P-1} \sum_{k=0}^{Q-1} \sum_n b_{k,n}^{(l)} c_k^{(l)}(t - nT) \tag{26}$$

where $c_k^{(l)}(t)$ are obtained from (7) and (8) with the modulation index $h^{(l)} = 2^l h$ and the pseudo-symbols $b_{k,n}^{(l)}$ are computed from (10) by replacing $\{\alpha_i\}$ with $\{\gamma_{i,l}\}$, i.e.

$$c_k^{(l)}(t) = \prod_{i=0}^{L-1} u^{(l)}(t + iT + \beta_{k,i} LT), \qquad 0 \leq k \leq Q-1 \tag{27}$$

$$u^{(l)}(t) = \begin{cases} \sin[2h^{(l)} \pi q(t)] / \sin(h^{(l)} \pi), & 0 \leq t \leq LT \\ u^{(l)}(2LT - t), & LT < t \leq 2LT \\ 0, & \text{elsewhere} \end{cases} \tag{28}$$

$$b_{k,n}^{(l)} = \exp\left\{ j h^{(l)} \pi \left[\sum_{m=-\infty}^{n} \gamma_{m,l} - \sum_{i=0}^{L-1} \gamma_{n-i,l} \beta_{k,i} \right] \right\}. \tag{29}$$

The next step consists of performing the products indicated in (26). Since this is a time-consuming task, detailed passages are not given[1] and only the final results are illustrated. They are summarized in the following equation which extends Laurent formula (6) to multilevel modulations

$$s(t, \boldsymbol{\alpha}) = \sum_{k=0}^{N-1} \sum_n a_{k,n} g_k(t - nT), \qquad N = Q^P(2^P - 1). \tag{30}$$

Key quantities in (30) are the $g_k(t)$, henceforth called *Laurent functions* (LF's), and the pseudo-symbols $a_{k,n}$. These quantities are described below.

C. Computing $g_k(t)$ and $a_{k,n}$

Let us start with a few notations. First, we consider the radix-Q representation of an integer j belonging to the interval $0 \leq j \leq Q^P - 1$

$$j = \sum_{l=0}^{P-1} Q^l d_{j,l}, \qquad 0 \leq j \leq Q^P - 1, \quad d_{j,l} \in \{0, 1, \cdots, Q-1\} \tag{31}$$

[1] Working notes will be provided to the interested reader on request.

and we collect the coefficients $d_{j,l}$ into a vector $\boldsymbol{d_j}$ as follows:

$$\boldsymbol{d_j} = \{d_{j,P-1}, d_{j,P-2}, \cdots, d_{j,0}\}. \tag{32}$$

Second, for each pair (j, l), we pick up the corresponding $d_{j,l}$ and we use it as a subscript to $c^{(l)}_{d_{j,l}}(t)$ defined in (27). Third, calling $D_{j,l}$ the duration of $c^{(l)}_{d_{j,l}}(t)$ (see (12)) and letting l vary in the interval $0 \le l \le P-1$, we form the vector

$$\boldsymbol{D_j} = \{D_{j,P-1}, D_{j,P-2}, \cdots, D_{j,0}\}. \tag{33}$$

Fourth, for a given $\boldsymbol{D_j}$, we seek the P-tuples

$$\boldsymbol{e^{(m)}_j} = \{e^{(m)}_{j,P-1}, e^{(m)}_{j,P-2}, \cdots, e^{(m)}_{j,0}\}, \qquad m = 0, 1, 2, \cdots \tag{34}$$

with integer components and satisfying the equations

$$0 \le e^{(m)}_{j,l} \le D_{j,l} - 1, \qquad 0 \le l \le P-1, \tag{35}$$

$$\prod_{l=0}^{P-1} e^{(m)}_{j,l} = 0. \tag{36}$$

It can be shown that there are $\mathcal{M}_j$ such P-tuples, where $\mathcal{M}_j$ is given by

$$\mathcal{M}_j = \prod_{l=0}^{P-1} D_{j,l} - \prod_{l=0}^{P-1} (D_{j,l} - 1). \tag{37}$$

At this stage the computation of $g_k(t)$ and $a_{k,n}$ proceeds as follows. For each j we consider the functions

$$h^{(m)}_j(t) = \prod_{l=0}^{P-1} c^{(l)}_{d_{j,l}}(t + e^{(m)}_{j,l} T), \qquad 0 \le m \le \mathcal{M}_j - 1. \tag{38}$$

As j varies in the interval $0 \le j \le Q^P - 1$, $h^{(m)}_j(t)$ spans a set containing $N = \mathcal{M}_0 + \mathcal{M}_1 + \cdots + \mathcal{M}_{Q^P-1} = Q^P(2^P - 1)$ elements. This is just the set of the Laurent functions. For convenience we order the elements in the set by establishing the following map $(j, m) \rightarrow k$ between pairs (j, m) and subscripts k to $g_k(t)$

$$k = m + \sum_{n=0}^{j-1} \mathcal{M}_n, \qquad 0 \le j \le Q^P - 1, \quad 0 \le m \le \mathcal{M}_j - 1. \tag{39}$$

This leads to

$$g_k(t) = \prod_{l=0}^{P-1} c^{(l)}_{d_{j,l}}(t + e^{(m)}_{j,l} T) \tag{40}$$

and to the following expression for the pseudo-symbols

$$a_{k,n} = \prod_{l=0}^{P-1} b^{(l)}_{d_{j,l}, n - e^{(m)}_{j,l}}. \tag{41}$$

It is worth noting that, since the $c^{(l)}_k(t)$ are time-limited (see (13)), so are the LF's in (40). In fact, their duration (in symbol periods) is found to be an integer in the range $(1, L+1)$. Table II indicates how many LF's have a given duration. In the next Section we illustrate LD with a few examples.

TABLE II
PULSE DURATION

Duration	Number of $g_k(t)$
$L+1$	1
L	$2^P - 2$
$L-1$	$(2^P - 1)^2$
$L-2$	$2^P(2^P - 1)^2$
$L-3$	$2^{2P}(2^P - 1)^2$
.	.
.	.
1	$2^{(L-2)P}(2^P - 1)^2$

IV. EXAMPLES

A. Full Response Systems

With full response systems the memory L is unity and $Q = 2^{L-1} = 1$. Hence, the index j in (31) takes on the only value zero. Also, from (31) and (32) we see that

$$\boldsymbol{d_0} = \underbrace{\{0, 0, \cdots, 0\}}_{P \text{ times}}. \tag{42}$$

It follows that the pulses $c^{(l)}_{d_{j,l}}(t)$ in (38) belong to the set $\{c^{(l)}_0(t),\ 0 \le l \le P-1\}$. On the other hand, the functions in this set have all a duration equal to 2 (see (13)). Then, from (33) it follows that

$$\boldsymbol{D_0} = \underbrace{\{2, 2, \cdots, 2\}}_{P \text{ times}} \tag{43}$$

and, from (37), that $\mathcal{M}_0 = 2^P - 1$.

Equation (38) gives

$$h^{(m)}_0(t) = \prod_{l=0}^{P-1} c^{(l)}_0(t + e^{(m)}_{0,l} T), \qquad 0 \le m \le 2^P - 2 \tag{44}$$

where the coefficients $e^{(m)}_{0,l}$ satisfy (see (35) and (36))

$$e^{(m)}_{0,l} = \text{either } 0 \text{ or } 1 \tag{45}$$

$$\prod_{l=0}^{P-1} e^{(m)}_{0,l} = 0. \tag{46}$$

Finally, LF's and pseudo-symbols $a_{k,n}$ are derived from (40) and (41). As the index j is zero, (39) gives $k = m$ and we have

$$g_k(t) = \prod_{l=0}^{P-1} c^{(l)}_0(t + e^{(k)}_{0,l} T), \qquad 0 \le k \le 2^P - 2 \tag{47}$$

$$a_{k,n} = \prod_{l=0}^{P-1} b^{(l)}_{0, n - e^{(k)}_{0,l}}, \qquad 0 \le k \le 2^P - 2. \tag{48}$$

It turns out that the duration of $g_0(t)$ is 2 while it is unity for all the other $g_k(t)$. Tables III and IV provide expressions of $g_k(t)$ and $a_{k,n}$ for $M = 4$ and $M = 8$, respectively. Fig. 2 shows $c^{(0)}_0(t)$ and $c^{(1)}_0(t)$ for a $1REC$ frequency response and $h = 0.4$, while Fig. 3 illustrates the shape of $g_k(t)$ $(k = 0, 1, 2)$ for $M = 4$.

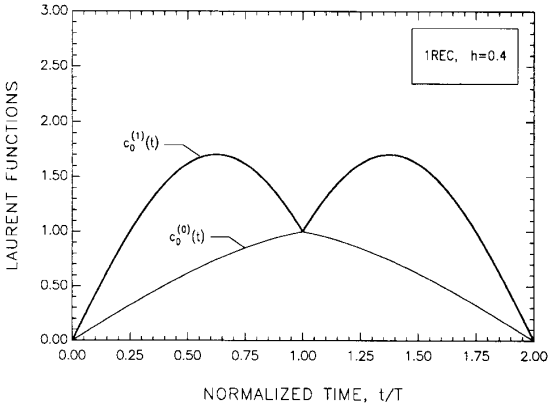

Fig. 2. Illustrating $c_0^{(0)}(t)$ and $c_0^{(1)}(t)$ for $1REC$ and $h = 0.4$.

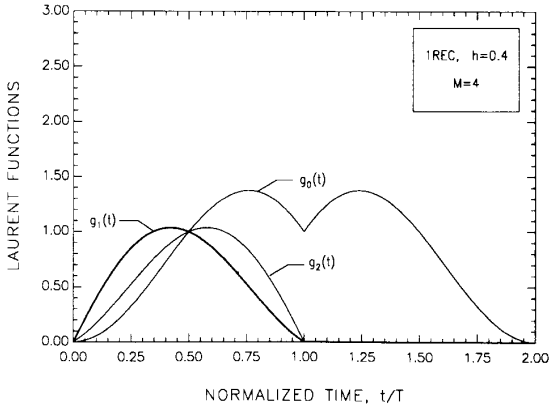

Fig. 3. Laurent functions for $1REC$, $h = 0.4$ and $M = 4$.

B. Quaternary Systems with $L = 2$

With a quaternary alphabet ($M = 4$) one has $P = 2$ (see (16)). Also, for $L = 2$, Q equals 2 (recall that $Q = 2^{L-1}$). Hence, the index j in (31) takes on values from 0 to 3. Let us consider these four cases separately:

1) $j = 0$: With the same arguments used above it is found

$$\boldsymbol{d_0} = \{0, 0\} \qquad \boldsymbol{D_0} = \{3, 3\} \qquad \mathcal{M}_0 = 5 \tag{49}$$

so that, from (38), we get

$$h_0^{(m)}(t) = c_0^{(0)}(t + e_{0,0}^{(m)}T)c_0^{(1)}(t + e_{0,1}^{(m)}T), \quad 0 \le m \le 4 \tag{50}$$

where $e_{0,0}^{(m)}$ and $e_{0,1}^{(m)}$ satisfy the equations

$$0 \le e_{0,0}^{(m)}, \qquad e_{0,1}^{(m)} \le 2 \tag{51}$$

$$e_{0,0}^{(m)} e_{0,1}^{(m)} = 0. \tag{52}$$

2) $j = 1$: Similarly, it is found

$$\boldsymbol{d_1} = \{0, 1\} \qquad \boldsymbol{D_1} = \{3, 1\} \qquad \mathcal{M}_1 = 3. \tag{53}$$

Hence, from (38) it follows that

$$h_1^{(m)}(t) = c_1^{(0)}(t + e_{1,0}^{(m)}T)c_0^{(1)}(t + e_{1,1}^{(m)}T), \quad 0 \le m \le 2 \tag{54}$$

TABLE III
LAURENT FUNCTIONS FOR $M = 4$, $L = 1$

k	$e_{0,1}^{(k)}$	$e_{0,0}^{(k)}$	$g_k(t)$	$a_{k,n}$
0	0	0	$c_0^{(0)}(t)\, c_0^{(1)}(t)$	$b_{0,n}^{(0)}\, b_{0,n}^{(1)}$
1	0	1	$c_0^{(0)}(t+T)\, c_0^{(1)}(t)$	$b_{0,n-1}^{(0)}\, b_{0,n}^{(1)}$
2	1	0	$c_0^{(0)}(t)\, c_0^{(1)}(t+T)$	$b_{0,n}^{(0)}\, b_{0,n-1}^{(1)}$

TABLE IV
LAURENT FUNCTIONS FOR $M = 8$, $L = 1$

k	$e_{0,2}^{(k)}$	$e_{0,1}^{(k)}$	$e_{0,0}^{(k)}$	$g_k(t)$	$a_{k,n}$
0	0	0	0	$c_0^{(0)}(t)\, c_0^{(1)}(t)\, c_0^{(2)}(t)$	$b_{0,n}^{(0)}\, b_{0,n}^{(1)}\, b_{0,n}^{(2)}$
1	0	0	1	$c_0^{(0)}(t+T)\, c_0^{(1)}(t)\, c_0^{(2)}(t)$	$b_{0,n-1}^{(0)}\, b_{0,n}^{(1)}\, b_{0,n}^{(2)}$
2	0	1	0	$c_0^{(0)}(t)\, c_0^{(1)}(t+T)\, c_0^{(2)}(t)$	$b_{0,n}^{(0)}\, b_{0,n-1}^{(1)}\, b_{0,n}^{(2)}$
3	0	1	1	$c_0^{(0)}(t+T)\, c_0^{(1)}(t+T)\, c_0^{(2)}(t)$	$b_{0,n-1}^{(0)}\, b_{0,n-1}^{(1)}\, b_{0,n}^{(2)}$
4	1	0	0	$c_0^{(0)}(t)\, c_0^{(1)}(t)\, c_0^{(2)}(t+T)$	$b_{0,n}^{(0)}\, b_{0,n}^{(1)}\, b_{0,n-1}^{(2)}$
5	1	0	1	$c_0^{(0)}(t+T)\, c_0^{(1)}(t)\, c_0^{(2)}(t+T)$	$b_{0,n-1}^{(0)}\, b_{0,n}^{(1)}\, b_{0,n-1}^{(2)}$
6	1	1	0	$c_0^{(0)}(t)\, c_0^{(1)}(t+T)\, c_0^{(2)}(t+T)$	$b_{0,n}^{(0)}\, b_{0,n-1}^{(1)}\, b_{0,n-1}^{(2)}$

with

$$e_{1,0}^{(m)} = 0 \tag{55}$$

$$0 \le e_{1,1}^{(m)} \le 2. \tag{56}$$

3) $j = 2$: It is found that

$$\boldsymbol{d_2} = \{1, 0\} \qquad \boldsymbol{D_2} = \{1, 3\} \qquad \mathcal{M}_2 = 3. \tag{57}$$

Hence

$$h_2^{(m)}(t) = c_0^{(0)}(t + e_{2,0}^{(m)}T)c_1^{(1)}(t + e_{2,1}^{(m)}T), \quad 0 \le m \le 2 \tag{58}$$

where $e_{2,0}^{(m)}$ and $e_{2,1}^{(m)}$ satisfy the equations

$$0 \le e_{2,0}^{(m)} \le 2 \tag{59}$$

$$e_{2,1}^{(m)} = 0. \tag{60}$$

4) $j = 3$: It is found that

$$\boldsymbol{d_3} = \{1, 1\} \qquad \boldsymbol{D_3} = \{1, 1\} \qquad \mathcal{M}_3 = 1. \tag{61}$$

The only case to consider in (38) is $m = 0$. On the other hand, solving (35) and (36) yields

$$e_{3,0}^{(0)} = e_{3,1}^{(0)} = 0. \tag{62}$$

Hence, from (38) we obtain

$$h_3^{(0)}(t) = c_1^{(0)}(t)c_1^{(1)}(t). \tag{63}$$

Inserting the above results into (40) gives the expressions of the LF's. Table V provides expressions of $g_k(t)$ and $a_{k,n}$ for $M = 4$ and $L = 2$, while Fig. 4 illustrates the shape of these functions for the modulation index $h = 0.25$. It appears that $g_0(t)$, $g_1(t)$, and $g_2(t)$ have comparable amplitudes while the others are much smaller.

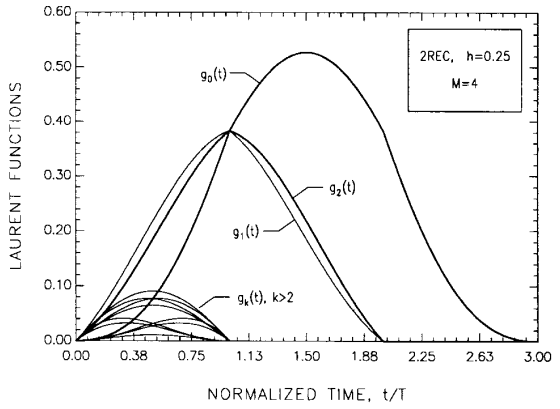

Fig. 4. Laurent functions for $2REC$, $h = 0.25$ and $M = 4$.

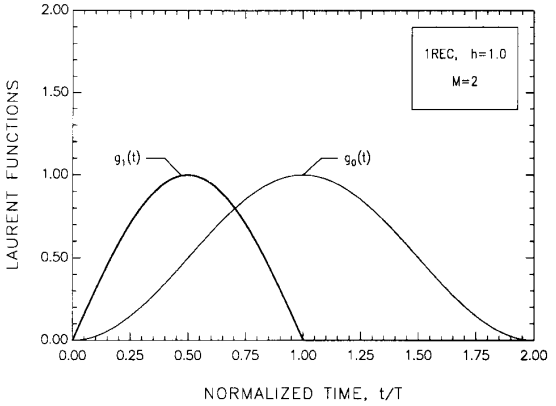

Fig. 5. Laurent functions for $1REC$, $h = 1.0$ and $M = 2$.

TABLE V
LAURENT FUNCTIONS FOR $M = 4$, $L = 2$

k	j	m	$\mathbf{e}_j^{(m)}$		$g_k(t)$	$a_{k,n}$
0		0	0	0	$c_0^{(0)}(t)\,c_0^{(1)}(t)$	$b_{0,n}^{(0)}\,b_{0,n}^{(1)}$
1		1	0	1	$c_0^{(0)}(t+T)\,c_0^{(1)}(t)$	$b_{0,n-1}^{(0)}\,b_{0,n}^{(1)}$
2	0	2	1	0	$c_0^{(0)}(t)\,c_0^{(1)}(t+T)$	$b_{0,n}^{(0)}\,b_{0,n-1}^{(1)}$
3		3	0	2	$c_0^{(0)}(t+2T)\,c_0^{(1)}(t)$	$b_{0,n-2}^{(0)}\,b_{0,n}^{(1)}$
4		4	2	0	$c_0^{(0)}(t)\,c_0^{(1)}(t+2T)$	$b_{0,n}^{(0)}\,b_{0,n-2}^{(1)}$
5		0	0	0	$c_1^{(0)}(t)\,c_0^{(1)}(t)$	$b_{1,n}^{(0)}\,b_{0,n}^{(1)}$
6	1	1	1	0	$c_1^{(0)}(t)\,c_0^{(1)}(t+T)$	$b_{1,n}^{(0)}\,b_{0,n-1}^{(1)}$
7		2	2	0	$c_1^{(0)}(t)\,c_0^{(1)}(t+2T)$	$b_{1,n}^{(0)}\,b_{0,n-2}^{(1)}$
8		0	0	0	$c_0^{(0)}(t)\,c_1^{(1)}(t)$	$b_{0,n}^{(0)}\,b_{1,n}^{(1)}$
9	2	1	0	1	$c_0^{(0)}(t+T)\,c_1^{(1)}(t)$	$b_{0,n-1}^{(0)}\,b_{1,n}^{(1)}$
10		2	0	2	$c_0^{(0)}(t+2T)\,c_1^{(1)}(t)$	$b_{0,n-2}^{(0)}\,b_{1,n}^{(1)}$
11	3	0	0	0	$c_1^{(0)}(t)\,c_1^{(1)}(t)$	$b_{1,n}^{(0)}\,b_{1,n}^{(1)}$

C. Full Response Binary Systems with $h = 1$

In Section II it has been pointed out that, with a binary alphabet and a modulation index equal to one, LD seems to fail because the denominator of the function $u(t)$ in (8) vanishes. On the other hand, it is easily seen that a signal $s(t, \boldsymbol{\alpha})$ with $h = 1$ may be thought of as the product of two CPM signals with $h = 1/2$, i.e.

$$s(t, \boldsymbol{\alpha}) = \exp\left[j\pi\sum_i \alpha_i q(t - iT)\right] \times \exp\left[j\pi\sum_i \alpha_i q(t - iT)\right]. \quad (64)$$

Thus application of LD to each factor in (64) yields

$$s(t, \boldsymbol{\alpha}) = \left\{\sum_n b_{0,n} c_0(t - nT)\right\}^2 = \sum_n\sum_k b_{0,n} b_{0,k} c_0(t - nT) c_0(t - kT) \quad (65)$$

TABLE VI
LAURENT FUNCTIONS FOR $M = 2$, $L = 1$, $h = 1$

k	$g_k(t)$	$a_{k,n}$
0	$c_0^2(t)$	$(-1)^n$
1	$2c_0(t)c_0(t+T)$	$-j(-1)^n\alpha_n$

where, as a consequence of (7) and (10), one has

$$c_0(t) = \begin{cases} \sin[\pi q(t)], & 0 \le t \le T \\ c_0(2T - t), & T < t \le 2T \\ 0, & \text{elsewhere} \end{cases} \quad (66)$$

$$b_{0,n} = \exp\left\{j\frac{\pi}{2}\sum_{m=-\infty}^{n}\alpha_m\right\}. \quad (67)$$

Next, bearing in mind that $c_0(t)$ has a duration equal to 2, with simple manipulations (65) is transformed into

$$s(t, \boldsymbol{\alpha}) = \sum_n a_{0,n} g_0(t - nT) + \sum_n a_{1,n} g_1(t - nT) \quad (68)$$

where $g_0(t)$ and $g_1(t)$ and the pseudo-symbols $a_{0,n}$ and $a_{1,n}$ are as given in Table VI. In particular, as $a_{0,n}$ equals $(-1)^n$, it is recognized that the first sum in (68) is periodic of period $2T$. Of course, this reflects the lines in the spectrum of a binary signal with $h = 1$ [2, ch. 4]. Fig. 5 shows the shape of $g_0(t)$ and $g_1(t)$.

D. Full Response Systems with $M = 4$ and $h = 1/2$

Application of (23) and (25) for $M = 4$ and $h = 1/2$ yields $s(t, \boldsymbol{\alpha})$ as a product of two binary signals, with modulation indexes 1/2 and 1, respectively, i.e.

$$s(t, \boldsymbol{\alpha}) = \exp\left[j\pi\sum_i \gamma_{i,0} q(t - iT)\right] \times \exp\left[j2\pi\sum_i \gamma_{i,1} q(t - iT)\right]. \quad (69)$$

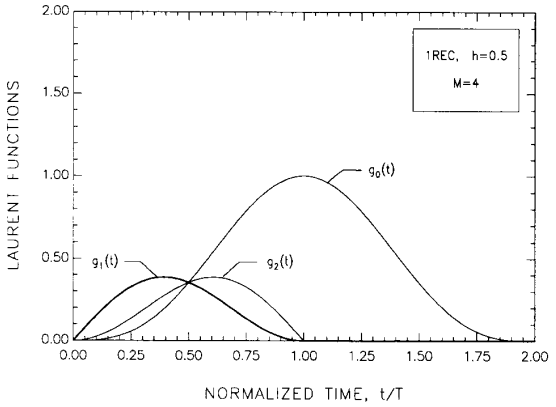

Fig. 6. Laurent functions for $1REC$, $h = 0.5$ and $M = 4$.

Next, making use of the results of the previous subsection, (69) is transformed into

$$s(t, \boldsymbol{\alpha}) = \left[\sum_n b_{0,n} c_0(t - nT)\right] \times \left[\sum_n (-1)^n c_0^2(t - nT) - 2j \sum_n (-1)^n \gamma_{n,1} c_0(t - nT) c_0(t - nT + T)\right] \tag{70}$$

with $c_0(t)$ and $b_{0,n}$ as given in (27) and (29). In particular, bearing in mind that $c_0(t)$ is time-limited, after some algebra (70) becomes

$$s(t, \boldsymbol{\alpha}) = \sum_{k=0}^{2} a_{k,n} g_k(t - nT) \tag{71}$$

where $g_k(t)$ and $a_{k,n}$ are described in Table VII. Fig. 6 shows the form of $g_0(t)$, $g_1(t)$, and $g_2(t)$.

V. Approximate Laurent Decomposition

A. Mean-Square Approximation

It has been seen that a CPM signal can be decomposed into the sum of $N = Q^P(2^P - 1)$ PAM waveforms. Through extensive numerical calculations we have found that, in most cases, the signal power is unevenly distributed between these waveforms and, indeed, it is consistently concentrated only in some of them. In particular, letting $\mathcal{N}_0 = 2^P - 1$, it turns out that the most important waveforms are associated with the following LF's:

$$g_k(t) = \sum_{l=0}^{P-1} c_0^{(l)}(t + e_{0,l}^{(k)} T), \qquad 0 \le k \le \mathcal{N}_0 - 1 \tag{72}$$

wherein the coefficients $e_{0,l}^{(k)}$ satisfy the equations

$$e_{0,l}^{(k)} = \text{either } 0 \text{ or } 1 \tag{73}$$

$$\prod_{l=0}^{P-1} e_{0,l}^{(k)} = 0. \tag{74}$$

This fact is illustrated in Fig. 4 for $L = 2$ and $M = 4$. In this case we have $\mathcal{N}_0 = 3$, and, indeed, it is seen that the first three LF's are the most significant ones.

In the sequel, (72) are denoted *principal* LF's and the corresponding PAM waveforms are referred to as *principal* Laurent components (LC's) of the CPM scheme. Note that in full response systems one has $L = Q = 1$ and therefore $N = \mathcal{N}_0$; in other words, *all the pulses are principal.*

Since the principal LC's, as a whole, contain most of the signal power, it is expected that their sum

$$\tilde{s}(t, \boldsymbol{\alpha}) = \sum_{k=0}^{\mathcal{N}_0 - 1} \sum_n a_{k,n} g_k(t - nT) \tag{75}$$

represents a good approximation to the complete LD in (30). Clearly, what makes (75) appealing compared with (30) is its reduced number of terms. For example, for a quaternary system with $L = 3$, the complete LD has $N = 48$ components while (75) has only $\mathcal{N}_0 = 3$ components.

An important question, however, is whether (75) is the best approximation we can get with only $\mathcal{N}_0$ components. As we will see shortly, this is not the case and, indeed, better results are obtained if pulses other than $g_k(t)$ are used in (75). This issue is addressed next.

Consider the sum

$$\hat{s}(t, \boldsymbol{\alpha}) = \sum_{k=0}^{\mathcal{N}_0 - 1} \sum_n a_{k,n} p_k(t - nT) \tag{76}$$

wherein the pseudo-symbols $\{a_{k,n}\}$ are the same as in (75) but the pulses $\{p_k(t)\}$ are arbitrary. We want to determine $\{p_k(t)\}$ so as to minimize the normalized mean-square error (MSE) between the complete LD and its approximation (76). In other terms, we seek the minimum of

$$\hat{\sigma}^2 = \frac{\int_0^T E\{|\hat{s}(t, \boldsymbol{\alpha}) - s(t, \boldsymbol{\alpha})|^2\}\, dt}{\int_0^T E\{|s(t, \boldsymbol{\alpha})|^2\}\, dt} = \frac{1}{T} \int_0^T E\{|\hat{s}(t, \boldsymbol{\alpha}) - s(t, \boldsymbol{\alpha})|^2\}\, dt \tag{77}$$

where the second line follows from the signal model (1). This minimum can be pursued by extending the methods in [13]. Since the derivation is long, we only provide the final results. Details are given in the Appendix.

The optimum pulse $p_k(t)$ is found as the sum of the corresponding principal LF $g_k(t)$ plus a combination of delayed versions of nonprincipal LF's, i.e.

$$p_k(t) = g_k(t) + \sum_{i=\mathcal{N}_0}^{N-1} \sum_m w_{k,i}(m) g_i(t - mT), \qquad 0 \le k \le \mathcal{N}_0 - 1 \tag{78}$$

where $w_{k,i}(m)$ are weights which are computed in the following manner. Call $A_{k,i}(l) = E\{a_{k,n} a_{i,n+l}^*\}$ the autocorrelation of the pseudo-symbols, and $\mathcal{A}_{k,i}(f)$ the associated

TABLE VII
LAURENT FUNCTIONS FOR $M = 4$, $L = 1$, $h = 0.5$

k	$g_k(t)$	$a_{k,n}$
0	$c_0^3(t)$	$\exp\left\{j\frac{\pi}{2}\sum_{m=-\infty}^{n}\alpha_m\right\}$
1	$c_0(t)c_0^2(t+T)$	$j\alpha_n\, a_{0,n-1}$
2	$c_0^2(t)c_0(t+T)$	$-j\alpha_n\, a_{0,n}$

spectrum, i.e., the discrete Fourier transform (DFT) of $A_{k,i}(l)$

$$\mathcal{A}_{k,i}(f) = \sum_l A_{k,i}(l)e^{-j2\pi lfT}. \tag{79}$$

Also, denote $\mathbf{A}(f)$ the $\mathcal{N}_0 \times \mathcal{N}_0$ matrix with (i, j)-entry equal to $\mathcal{A}_{i,j}(f)$, and $\mathbf{B}(f)$ the $\mathcal{N}_0 \times (N - \mathcal{N}_0)$ matrix with (i, j)-entry equal to $\mathcal{A}_{i,j+\mathcal{N}_0}(f)$, i.e.

$$\mathbf{A}(f) = \{\mathcal{A}_{i,j}(f)\}, \qquad 0 \le i, j \le \mathcal{N}_0 - 1 \tag{80}$$

$$\mathbf{B}(f) = \{\mathcal{A}_{i,j+\mathcal{N}_0}(f)\}, \qquad 0 \le i \le \mathcal{N}_0 - 1, \quad 0 \le j \le N - \mathcal{N}_0 - 1. \tag{81}$$

The weights in (78) are obtained through the following steps. First, one computes the $\mathcal{N}_0 \times (N - \mathcal{N}_0)$ matrix $\mathbf{C}(f) = \{\mathcal{C}_{i,j}(f)\}$, related to $\mathbf{A}(f)$ and $\mathbf{B}(f)$ by

$$\mathbf{C}(f) = \mathbf{A}^{-1}(f) \times \mathbf{B}(f) \tag{82}$$

where $\mathbf{A}^{-1}(f)$ is the inverse of $\mathbf{A}(f)$. Second, by renumerating the columns of $\mathbf{C}(f)$, one gets the matrix $\mathbf{W}(f) = \{\mathcal{W}_{i,j}(f)\}$ with entries

$$\mathcal{W}_{i,j}(f) = \mathcal{C}_{i,j-\mathcal{N}_0}(f), \qquad 0 \le i \le \mathcal{N}_0 - 1, \quad \mathcal{N}_0 \le j \le N - 1. \tag{83}$$

Finally, the generic weight $w_{k,i}(m)$ is computed as the inverse DFT of $\mathcal{W}_{k,i}(f)$, i.e.

$$w_{k,i}(n) = T\int_{-1/2T}^{1/2T} \mathcal{W}_{k,i}(f)e^{j2\pi nfT}\, df. \tag{84}$$

Since the $w_{k,i}(m)$ are functions of the correlations $A_{k,i}(l)$, it is important to see how these correlations are computed. We concentrate on the important case where the size M of the signal alphabet is a power of two, say $M = 2^P$ (see (16)). As we mentioned in Section III, in this case the subsequences $\{\gamma_{i,l}\}$ $(0 \le l \le P - 1)$ derived from the information data $\{\alpha_i\}$ are all independent. It follows that the same is true with the sequences $\{b_{k,n}^{(l)}\}$ $(0 \le l \le P - 1)$ defined in (29). Then, it appears from (41) that $A_{k,i}(l)$ results in the product of P factors of the type

$$B_{i,j}^{(l)}(q) = E\{b_{i,k}^{(l)} b_{j,k+q}^{(l)*}\} \qquad (0 \le l \le P - 1).$$

They represent the correlations of the sequences $\{b_{k,n}^{(l)}\}$ and can be computed from (14) and (15) by replacing the modulation index h with $h^{(l)} = 2^l h$.

One last important point is to know how good the MSE approximation (77) is. The answer is obtained by substituting (30) and (76) into (77). As a result we get the *residual* MSE in the form

$$\hat{\sigma}_{\text{res}}^2 = \frac{1}{T}\sum_{i=0}^{N-1}\sum_{j=0}^{N-1}\sum_l A_{i,j}(l)\int_{-\infty}^{\infty} z_i(t)z_j(t - lT)\, dt \tag{85}$$

where $z_k(t)$ is defined as

$$z_k(t) = \begin{cases} g_k(t) - p_k(t), & 0 \le k \le \mathcal{N}_0 - 1 \\ g_k(t), & \text{otherwise.} \end{cases} \tag{86}$$

A few examples illustrating the MSE approximation are discussed next.

VI. FURTHER EXAMPLES

A. Binary Systems with $L = 2$

For $L = 2$ one has $Q = 2^{L-1} = 2$. Also, since $M = 2$, from (16) one gets $P = 1$. It follows that the complete LD in (30) has $N = Q^P(2^P - 1) = 2$ components while its approximation (76) has only one component (indeed, $\mathcal{N}_0 = 2^P - 1 = 1$). Such a component is characterized by a pulse $p_0(t)$ which is obtained from (78)

$$p_0(t) = g_0(t) + \sum_m w_{0,1}(m)g_1(t - mT). \tag{87}$$

Since the computation of $\{g_k(t)\}$ has already been illustrated in Section IV, in the sequel we concentrate on the weights $w_{0,1}(m)$. To this end let us start from the matrix $\mathbf{C}(f)$ in (82) which, in the present case, reduces to a scalar $\mathcal{C}_{0,0}(f)$, given by

$$\mathcal{C}_{0,0}(f) = \frac{\mathcal{A}_{0,1}(f)}{\mathcal{A}_{0,0}(f)}. \tag{88}$$

Thus from (83) we have the DFT of $w_{0,1}(m)$ in the form

$$\mathcal{W}_{0,1}(f) = \frac{\mathcal{A}_{0,1}(f)}{\mathcal{A}_{0,0}(f)}. \tag{89}$$

To get $\mathcal{A}_{0,0}(f)$ and $\mathcal{A}_{0,1}(f)$ we need the correlations $A_{0,0}(l)$ and $A_{0,1}(l)$. Letting

$$\rho = \cos(h\pi) \tag{90}$$

from (14) and (15) it is found that

$$A_{0,0}(l) = \rho^{|l|} \tag{91}$$

$$A_{0,1}(l) = \begin{cases} \rho^{1-l}, & l \le 0 \\ \rho^2, & l = 1 \\ \rho^{l-1}, & l \ge 2. \end{cases} \tag{92}$$

Hence, taking the DFT's of (91) and (92) and substituting the result into (89) yields

$$\mathcal{W}_{0,1}(f) = \rho[1 - \rho\exp(-j2\pi fT) + \exp(-j4\pi fT)] \tag{93}$$

from which the desired expression of $w_{0,1}(m)$ is obtained taking the inverse DFT

$$w_{0,1}(m) = \rho\delta(m) - \rho^2\delta(m - 1) + \rho\delta(m - 2) \tag{94}$$

where $\delta(m)$ is unity for $m = 0$ and is zero otherwise.

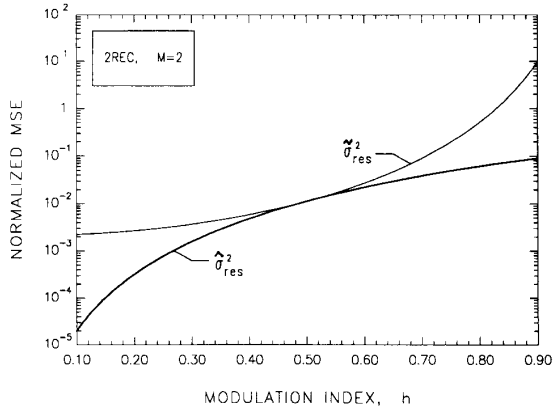

Fig. 7. Illustrating $\hat{\sigma}^2_{\rm res}$ and $\tilde{\sigma}^2_{\rm tr}$ as a function of the modulation index.

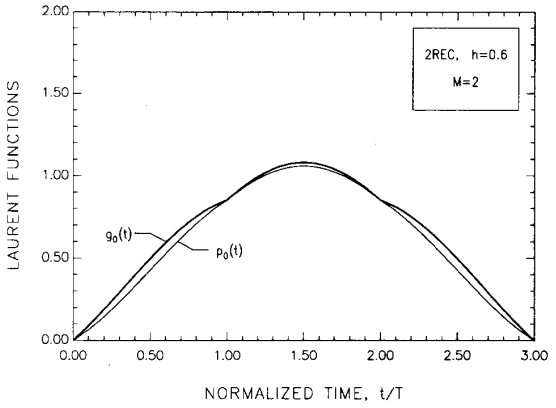

Fig. 8. $p_0(t)$ and $g_0(t)$ for $2REC$, $h = 0.6$ and $M = 2$.

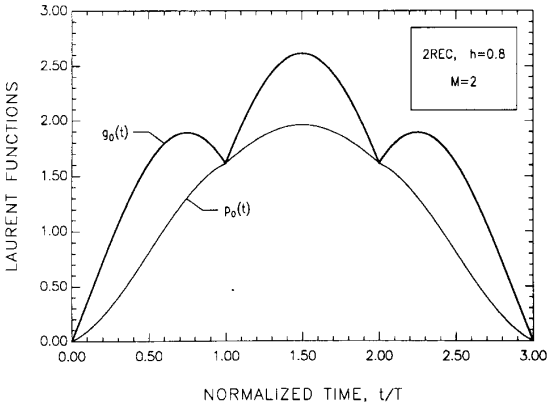

Fig. 9. $p_0(t)$ and $g_0(t)$ for $2REC$, $h = 0.8$ and $M = 2$.

Substituting into (87) results in

$$p_0(t) = g_0(t) + \rho g_1(t) - \rho^2 g_1(t-T) + \rho g_1(t-2T). \quad (95)$$

The residual MSE reads

$$\hat{\sigma}^2_{\rm res} = \frac{1}{T}\sin^4(h\pi)\int_0^T g_1^2(t)\,dt. \quad (96)$$

It is interesting to compare (96) with the MSE we incur by approximating the CPM signal with its principal Laurent components, as indicated in (75). As in the present case there is only one Laurent component ($\mathcal{N}_0 = 1$), the MSE is computed from (85) and (86) by replacing $p_0(t)$ with $g_0(t)$ and the result is

$$\tilde{\sigma}^2_{\rm res} = \frac{1}{T}\int_0^T g_1^2(t)\,dt \quad (97)$$

which is larger than $\hat{\sigma}^2_{\rm res}$ unless $h = 1/2$.

Fig. 7 shows $\hat{\sigma}^2_{\rm res}$ and $\tilde{\sigma}^2_{\rm res}$ as a function of h for a $2REC$ signaling scheme while Figs. 8 and 9 illustrate the shape of $p_0(t)$ and $g_0(t)$ for $h = 0.6$ and $h = 0.8$, respectively.

B. Quaternary System with $h = 1/4$ and $L = 2$

In this case the complete LD has $N = 12$ terms (see Table V) while its MSE approximation has $\mathcal{N}_0 = 3$ terms. The latter are associated with the pulses $p_k(t)$ $(k = 0, 1, 2)$ which are derived from (78). Again, we concentrate on the computation of the weights $\{w_{k,i}(m)\}$. Skipping the passages, the matrix $\mathbf{C}(f)$ is found to be (see (98) at the bottom of this page) where the shorthand notation $\lambda = e^{-j2\pi fT}$ has been used. Substituting into (83) yields $\mathbf{W}(f) = \{\mathcal{W}_{i,j}(f)\}$ from which the weights $\{w_{k,i}(m)\}$ are obtained through (84). The optimum pulses are found to be

$$p_0(t) = g_0(t) + g_5(t)/\sqrt{2} - g_6(t-T)/2 + g_7(t-2T)/\sqrt{2} \quad (99)$$

$$p_1(t) = g_1(t) + g_3(t)/\sqrt{2} + g_6(t-T)/\sqrt{2} \quad (100)$$

$$p_2(t) = g_2(t) + g_6(t)/\sqrt{2} + g_4(t-T)/\sqrt{2}. \quad (101)$$

Figs. 10–12 compare optimized versus principal pulses for a $2REC$ signaling scheme.

It can be shown that the residual MSE incurred by replacing $s(t, \boldsymbol{\alpha})$ with $\hat{s}(t, \boldsymbol{\alpha})$ in (76) is

$$\hat{\sigma}^2_{\rm res} = \frac{1}{T}\left[H_{3,3} + H_{5,5} + \frac{1}{4}H_{6,6} + 2H_{8,8} + H_{9,9} + H_{11,11} + \sqrt{2}H_{5,3} + 2\sqrt{2}(H_{9,8} + H_{11,8}) + H_{10,8} + H_{11,9}\right] \quad (102)$$

with

$$H_{i,j} = \int_{-\infty}^{\infty} g_i(t)g_j(t)\,dt. \quad (103)$$

$$\mathbf{C}(f) = \begin{bmatrix} 0 & 0 & 1/\sqrt{2} & -\lambda/2 & \lambda^2/\sqrt{2} & 0 & 0 & 0 & 0 \\ 1/\sqrt{2} & 0 & 0 & \lambda/\sqrt{2} & 0 & 0 & 0 & 0 & 0 \\ 0 & \lambda/\sqrt{2} & 0 & 1/\sqrt{2} & 0 & 0 & 0 & 0 & 0 \end{bmatrix} \quad (98)$$

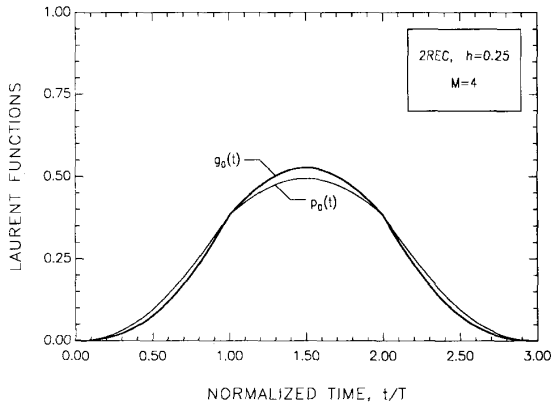

Fig. 10. $p_0(t)$ and $g_0(t)$ for $2REC$, $h = 0.25$ and $M = 4$.

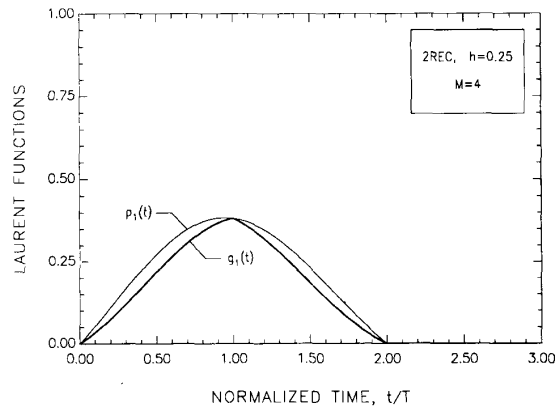

Fig. 11. $p_1(t)$ and $g_1(t)$ for $2REC$, $h = 0.25$ and $M = 4$.

Vice versa, by approximating $s(t, \boldsymbol{\alpha})$ with its principal Laurent components, one gets

$$\tilde{\sigma}^2_{\text{res}} = \frac{1}{T}[2H_{3,3} + 2H_{5,5} + H_{6,6} + 2H_{8,8} + H_{9,9} + H_{11,11} + 2\sqrt{2}(H_{5,3} + H_{9,8} + H_{11,8}) + H_{10,8} + H_{11,9}]. \quad (104)$$

Numerically it is found that $\hat{\sigma}^2_{\text{res}} = 1.67 \times 10^{-2}$ and $\tilde{\sigma}^2_{\text{res}} = 2.32 \times 10^{-2}$ with $2REC$ pulses, while $\hat{\sigma}^2_{\text{res}} = 2.06 \times 10^{-4}$ and $\tilde{\sigma}^2_{\text{res}} = 2.95 \times 10^{-4}$ with $2RC$ pulses.

VII. Conclusions

We have shown that a general M-ary CPM signal can be decomposed into the sum of PAM components. This result generalizes a previous statement which was limited to binary signaling. A general method has been described to compute Laurent functions and pseudo-symbols associated with each PAM component as a function of parameters such as modulation index, alphabet size, and frequency response of the system.

It has been pointed out that, especially for signaling schemes with a long memory, the number of PAM components may be large. For these cases, a reduced-complexity decomposition has been proposed which approximates the CPM signal in the minimum MSE sense. Several examples have been provided to illustrate exact and approximate decompositions.

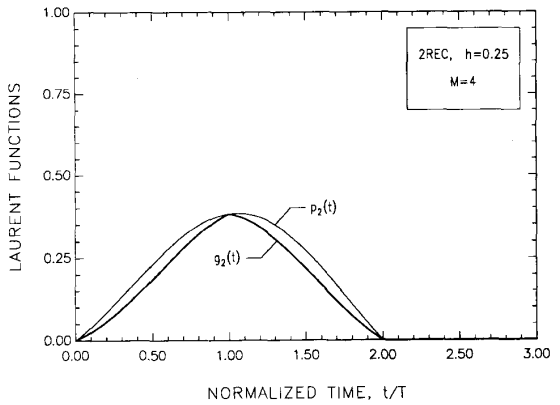

Fig. 12. $p_2(t)$ and $g_2(t)$ for $2REC$, $h = 0.25$ and $M = 4$.

Appendix

In this Appendix we derive the optimum pulses $p_k(t)$, $0 \le k \le \mathcal{N}_0 - 1$ that minimize the MSE

$$\hat{\sigma}^2 = \frac{1}{T}\int_0^T E\{|\hat{s}(t, \boldsymbol{\alpha}) - s(t, \boldsymbol{\alpha})|^2\}\, dt. \quad (A1)$$

As a starting point we note that minimizing (A1) amounts to minimizing the integrand

$$\sigma^2(t) = E\{|\hat{s}(t, \boldsymbol{\alpha}) - s(t, \boldsymbol{\alpha})|^2\} \quad (A2)$$

at each time t in the interval $0 \le t \le T$. Thus letting $p_k(n) = p_k(t + nT)$, $g_k(n) = g_k(t + nT)$, and setting to zero the derivatives of (A2) with respect to $p_k(m)$ yields

$$\sum_{i=0}^{\mathcal{N}_0-1}\sum_n A_{k,i}(m-n)p_i(n) = \sum_{i=0}^{N-1}\sum_n A_{k,i}(m-n)g_i(n) \quad (A3)$$

for $(-\infty < m < \infty,\ 0 \le k \le \mathcal{N}_0 - 1)$, where

$$A_{k,i}(l) = E\{a_{k,n}a^*_{i,n+l}\}$$

are the correlations of the pseudo-symbols.

Multiplying (A3) by $e^{-j2\pi mfT}$ and summing for $-\infty < m < \infty$ gives

$$\sum_{i=0}^{\mathcal{N}_0-1}\mathcal{A}_{k,i}(f)\mathcal{P}_i(f) = \sum_{i=0}^{N-1}\mathcal{A}_{k,i}(f)\mathcal{G}_i(f), \quad 0 \le k \le \mathcal{N}_0 - 1 \quad (A4)$$

where $\mathcal{A}_{k,i}(f)$, $\mathcal{P}_i(f)$, and $\mathcal{G}_i(f)$ are the DFT's of $A_{k,i}(l)$, $p_i(n)$, and $g_i(n)$, respectively. Alternatively, (A4) may be written in the form

$$\sum_{i=0}^{\mathcal{N}_0-1}\mathcal{A}_{k,i}(f)\mathcal{D}_i(f) = \sum_{i=\mathcal{N}_0}^{N-1}\mathcal{A}_{k,i}(f)\mathcal{G}_i(f), \quad 0 \le k \le \mathcal{N}_0 - 1 \quad (A5)$$

with

$$\mathcal{D}_i(f) = \mathcal{P}_i(f) - \mathcal{G}_i(f), \qquad 0 \le i \le \mathcal{N}_0 - 1. \quad (A6)$$

Next, we convert (A5) to a matrix form making use of (80) and (81) in the text and introducing the vectors

$$\mathbf{D}(f) = (\mathcal{D}_0(f), \mathcal{D}_1(f), \cdots, \mathcal{D}_{\mathcal{N}_0-1}(f)) \tag{A7}$$

$$\mathbf{H}(f) = (\mathcal{G}_{\mathcal{N}_0}(f), \mathcal{G}_{\mathcal{N}_0+1}(f), \cdots, \mathcal{G}_{N-1}(f)). \tag{A8}$$

Note that $\mathbf{D}(f)$ represents the unknowns in (A5). Substituting into (A5) yields

$$\mathbf{A}(f) \times \mathbf{D}(f) = \mathbf{B}(f) \times \mathbf{H}(f) \tag{A9}$$

from which we obtain $\mathbf{D}(f)$

$$\mathbf{D}(f) = \mathbf{C}(f) \times \mathbf{H}(f) \tag{A10}$$

with

$$\mathbf{C}(f) = \mathbf{A}^{-1}(f) \times \mathbf{B}(f). \tag{A11}$$

The generic component of $\mathbf{D}(f)$ is derived from (A8) and (A10)

$$\mathcal{D}_k(f) = \sum_{i=0}^{N-\mathcal{N}_0-1} \mathcal{C}_{k,i}(f)\mathcal{G}_{i+\mathcal{N}_0}(f), \qquad 0 \le k \le \mathcal{N}_0 - 1. \tag{A12}$$

Hence, bearing in mind (A6), we get

$$\mathcal{P}_k(f) = \mathcal{G}_k(f) + \sum_{i=\mathcal{N}_0}^{N-1} \mathcal{W}_{k,i}(f)\mathcal{G}_i(f) \tag{A13}$$

where the functions $\mathcal{W}_{k,i}(f)$ are defined in (83) of the text.

As a final step we take the inverse DFT of (A13). Recalling that $p_k(n) = p_k(t+nT)$ and $g_k(n) = g_k(t+nT)$ we arrive at

$$p_k(t) = g_k(t) + \sum_{i=\mathcal{N}_0}^{N-1} \sum_m w_{k,i}(m) g_i(t - mT), \qquad 0 \le k \le \mathcal{N}_0 - 1, \tag{A14}$$

which is the desired result.

REFERENCES

[1] J. B. Anderson and C.-E. W. Sundberg, "Advances in constant envelope coded modulation," *IEEE Commun. Mag.*, vol. 29, no. 12, pp. 36–45, Dec. 1991.

[2] J. B. Anderson, T. Aulin, and C.-E. W. Sundberg, *Digital Phase Modulation.* New York: Plenum, 1986.

[3] A. Svensson, T. Aulin, and C.-E. W. Sundberg, "A class of reduced complexity Viterbi detectors for partial response continuous phase modulation," *IEEE Trans. Commun.*, vol. COM-32, pp. 1079–1087, Oct. 1984.

[4] A. Svensson, "Reduced state sequence detection of partial response continuous phase modulation," *Proc. Inst. Elec. Eng.*, pt. I, vol. 138, no. 4, pp. 256–268, Aug. 1991.

[5] S. J. Simmons and P. H. Wittke, "Low complexity decoders for constant envelope digital modulations," *IEEE Trans. Commun.*, vol. COM-31, pp. 1273–1280, Dec. 1983.

[6] J. Huber and W. Liu, "An alternative approach to reduced complexity CPM receivers," *IEEE J. Selected Areas Commun.*, vol. 7, pp. 1437–1449, Sept. 1989.

[7] G. Kawas Kaleh, "Simple coherent receivers for partial response continuous phase modulation," *IEEE J. Selected Areas Commun.*, vol. 7, pp. 1427–1436, Sept. 1989.

[8] T. Palenius and A. Svensson, "Reduced complexity detectors for continuous phase modulation based on a signal space approach," *European Trans. Telecommun.*, vol. 4, no. 3, pp. 51–63, May–June 1993.

[9] R. de Buda, "Coherent demodulation of frequency shift keying with low deviation ratio," *IEEE Trans. Commun.*, vol. COM-20, pp. 429–435, June 1972.

[10] T. Aulin and C.-E. W. Sundberg, "Synchronization properties of continuous phase modulation," in *Proc. Int. Conf. on Communications* (Philadelphia, PA, June 1982), pp. D7.1.1–D7.1.7.

[11] M. K. Simon, "A generalization of minimum shift keying (MSK)-type signaling based upon input data symbol pulse shaping," *IEEE Trans. Commun.*, vol. COM-24, pp. 845–856, Aug. 1976.

[12] P. Galko and S. Pasupathy, "Linear receivers for correlative coded MSK," *IEEE Trans. Commun.*, vol. COM-33, pp. 338–347, Apr. 1985.

[13] P. A. Laurent, "Exact and approximate construction of digital phase modulations by superposition of amplitude modulated pulses," *IEEE Trans. Commun.*, vol. COM-34, pp. 150–160, 1986.

[14] G. Kawas Kaleh, "Differential detection via the Viterbi algorithm for offset modulation and MSK-type signals," *IEEE Trans. Veh. Technol.*, vol. 41, pp. 401–406, Nov. 1992.

[15] A. N. D'Andrea and U. Mengali, "Frequency detectors for CPM signals," accepted for publication in the *IEEE Trans. Commun.*